
**Separation Science and Technology**
Publication details, including instructions for authors and subscription information:
http://www.informaworld.com/smpp/title~content=t713708471

# Measurement of Adsorption Characteristics of Enantiomers on Chiral Columns: Comparison of the Frontal and Elution Chromatographic Techniques

Shih-Ming Lai[a]; Zi-Chin Lin[a]
[a] DEPARTMENT OF CHEMICAL ENGINEERING, NATIONAL YUNLIN UNIVERSITY OF SCIENCE AND TECHNOLOGY, YUNLIN, TAIWAN, REPUBLIC OF CHINA

Online publication date: 12 June 1999

**To cite this Article** Lai, Shih-Ming and Lin, Zi-Chin(1999) 'Measurement of Adsorption Characteristics of Enantiomers on Chiral Columns: Comparison of the Frontal and Elution Chromatographic Techniques', Separation Science and Technology, 34: 16, 3173 — 3196
**To link to this Article: DOI:** 10.1081/SS-100100829
**URL:** http://dx.doi.org/10.1081/SS-100100829

SEPARATION SCIENCE AND TECHNOLOGY, **34**(16), pp. 3173–3196, 1999

# Measurement of Adsorption Characteristics of Enantiomers on Chiral Columns: Comparison of the Frontal and Elution Chromatographic Techniques

SHIH-MING LAI* and ZI-CHIN LIN
DEPARTMENT OF CHEMICAL ENGINEERING
NATIONAL YUNLIN UNIVERSITY OF SCIENCE AND TECHNOLOGY
123, SEC. 3, UNIVERSITY ROAD, TOULIU, YUNLIN, TAIWAN, REPUBLIC OF CHINA



## ABSTRACT

This study measured the adsorption characteristics of 1,1′-bi-2-naphthol on Pirkle-type (3,5-dinitrobenzoyl phenylglycine covalently bonded to silica gel) chiral columns. The single-component isotherm of each isomer was measured by the elution on a plateau (EP) and the frontal analysis (FA) methods. The results showed that the *R*-isomer is more retained than the *S*-isomer, and the separation factor between them is about 1.1. The adsorption behavior of each isomer conforms to the Langmuir model in the concentration range studied. The isosteric heat of adsorption was constant regardless of the amount adsorbed for both the *R*-isomer and the *S*-isomer. These results suggest that Pirkle covalent D-phenylglycine has an energetically homogeneous surface. In contrast, the isotherm data obtained by the FA and EP methods are in good agreement with errors within about 5% for both components. The FA method was selected as the more rapid, precise, and accurate method for isotherm measurement. However, the EP method was used to measure the other adsorption characteristics, e.g., the axial dispersion coefficient and the diffusion coefficient of each solute, besides the equilibrium isotherm.

*Key Words.* Enatiomers; Chiral columns; Measurement of adsorption characteristics; Frontal chromatography; Elution chromatography

## INTRODUCTION

In recent years the separation of enantiomers has been an important issue in the fields of pharmacy, agrochemicals, food, petrochemicals, etc. For in-

* To whom correspondence should be addressed.

stance, in the health-related field, when it is well known that one of the enantiomers has a highly desirable therapeutic effect and the other has a different or sometimes undesirable effect, and further identification of the content of the necessary optically active material is strictly required by regulatory agencies. This situation has created a demand for preparative-scale techniques for the separation of enantiomers.

High performance liquid chromatography (HPLC) using chiral stationary phases (CSPs) is by far the most wildly used technique employed today for the effective and massive separations of enantiomers. Over 50 different CSPs are now commercially available. Based on the complexes between a solution and a stationary phase that are formed, they are classified into: (a) Brush- or Pirkle-type phases, (b) helical polymer phases, (c) cavity phases, (d) ligand-exchange phases, and (e) affinity phases. Of these, the Brush- or Pirkle-type is arguably the most versatile and selective (1, 2).



These enantio-separation systems can be operated by either the single-column elution chromatographic mode or the multicolumn simulated moving-bed (SMB) mode. However, the separation factors obtained for chiral separations are frequently very low, being of the order of 1.1 to 1.5 rather than the values of 5 to 10 or more which can be encountered in reverse-phase separations, which has thus caused difficulty in enantio-separation in preparative scale (2–4). Theoretical modeling and simulation can be used to predict the performance of these systems and to provide a helpful tool for design of scaled-up units and optimization of their operating conditions. The reliability of simulation has to be built on accurate adsorption characteristics, including the equilibrium and kinetic model parameters.

The separation of 1,1′-bi-2-naphthol enantiomers using Pirkle covalent D-phenylglycine (3,5-dinitrobenzoyl derivative of phenylglycine covalently bonded to aminopropyl silica gel) as the chiral stationary phase was investigated in this study. Optically pure enantiomers of 1,1′-bi-2-naphthol can be used as the chiral precursor of various optically active catalysts used in enantioselective syntheses of various optically active compounds with high optical purity (5). For example, the *R*-form of 1,1′-bi-2-naphthol forms a chiral boron-containing Lewis acid which has been used in asymmetric Diels–Alder reactions (6).

Liquid chromatography offers a dynamic method for accurate and rapid measurement of adsorption characteristics compared to the traditional shake-flask method (7, 8). Among the liquid chromatographic methods used, the elution on a plateau (EP) method (9–11) and the frontal analysis (FA) method (12–14) are mostly preferred. In this study the adsorption isotherms of the isomers of 1,1′-bi-2-naphthol (including the *R*-form and the *S*-form) were measured by the EP and FA methods and the kinetic parameters were measured by the EP method. A description of the two different methods of measurement



MARCEL DEKKER, INC.
270 Madison Avenue, New York, New York 10016

employed and a comparison between the results they provide will be presented in this paper.

## THEORY

### Model of Adsorption Behavior

Experimental data in this study have been correlated to the Langmuir equation for liquid–solid adsorption (15):

$$q = aC/(1 + bC) \tag{1}$$

where $q$ is the amount of adsorbate on one unit of adsorbent [mmol/mL of adsorbent (with pores)], $C$ is the solute concentration (mmol/mL of solution), parameter $b$ is an empirical constant related to the energy of adsorption (mL of solution/mmol), and parameter $a$ is the isotherm slope at low solute concentration [mL of solution/mL of adsorbent (with pores)] which can be expressed by

$$a = K_0 = dq/dC\,|_{c\to 0} \tag{2}$$

where $K_0$ is the particle-based equilibrium constant [mL of solution/mL of adsorbent (with pores)] in the domain of Henry's law.

The Langmuir model, which offers the greatest simplicity, convenience, and adequate correlation with available data, has been widely used to correlate data obtained in liquid–solid adsorption experiments.

### The Moment Method

A small perturbation pulse of a solute was injected to the steady flow of an eluent. The chromatographic data observed, which were in the symmetrical Gaussian distribution form, were analyzed by the moment method (15).

The differential equilibrium constant, $K$, which was defined as the local slope of the equilibrium curve, i.e., $K = dq/dC$, was related to the first moment, $\mu_1$, or the mean retention time, $t_r$, and was calculated as follows:

$$\mu_1 \text{ (or } t_r) = t_{or} + \frac{L}{v_s}[(1 - \varepsilon)K] \tag{3a}$$

or

$$\begin{aligned}\mu_1 \text{ (or } t_r) &= \frac{L}{v}[1 + F(\varepsilon_p + K)] \\ &= \frac{L}{v_s}[\varepsilon + (1 - \varepsilon)(\varepsilon_p + K)]\end{aligned} \tag{3b}$$

where $L$ is the column length (cm); $F = (1 - \varepsilon)/\varepsilon$ is the phase ratio [mL of adsorbent (with pores)/mL of solution]; $\varepsilon$ is the column porosity; $v$ and $v_s$ are

the interstitial and the superficial velocities, respectively (cm/min); $v_s = v\varepsilon$; and $t_{or}$ is the mean retention time of a nonadsorbable species (minutes).

The overall mass transfer coefficient and the axial dispersion coefficient were related to the second moment or the variance and were calculated as follows:

$$\text{HETP} = \frac{\sigma^2}{\mu_1^2} L = \frac{2D_L}{v} + 2v\left(\frac{\varepsilon}{1-\varepsilon}\right)\frac{1}{kK}\left[1 + \frac{\varepsilon}{(1-\varepsilon)K}\right]^{-2} \quad (4a)$$

where HETP is the height of theoretical plate (cm), $\sigma^2$ is the variance ($\text{min}^2$), $D_L$ is the axial dispersion coefficient ($\text{cm}^2$/min), and $k$ is the overall mass transfer coefficient (1/min). $D_L$ includes the molecular diffusion and the axial mixing, and it is expressed as follows (16):

$$D_L = \eta D_m + \lambda v \quad (5)$$

where $D_m$ is the molecular diffusion coefficient ($\text{cm}^2$/min), $\eta$ is the tortuosity factor (dimensionless), and $\lambda$ is the axial mixing constant (cm). The effect of molecular diffusion was assumed to be negligible for the liquid-phase adsorption systems. Therefore, Eq. (4a) can be simplified as follows:

$$\text{HETP} = \frac{\sigma^2}{\mu_1^2} L \cong 2\lambda + 2v\left(\frac{\varepsilon}{1-\varepsilon}\right)\frac{1}{kK}\left[1 + \frac{\varepsilon}{(1-\varepsilon)K}\right]^{-2} \quad (4b)$$

Lastly, $\mu_1$ and $\sigma^2$ were calculated by the peak position and the peak width of the Gaussian distributed chromatogram, respectively, as follows:

$$\mu_1 = \mu_{1,\text{exp}} - V_e/Q_f \quad (6)$$

$$\sigma^2 = W_{1/2}^2/5.54 \quad (7)$$

where $\mu_{1,\text{exp}}$ is the measured peak time (minutes), $V_e$ is the extracolumn volume between an injector and a column and between a column and a detector (mL), $Q_f$ is the volumetric flow rate of the eluent (mL/min), and $W_{1/2}$ is the peak width at half height (minutes).

## EXPERIMENTAL

### Materials

The separation of 1,1′-bi-2-naphthol enantiomers using Pirkle covalent D-phenylglycine (3,5-dinitrobenzoyl derivative of phenylglycine covalently bonded to aminopropyl silica gel) as chiral stationary phase and 50/15/1 (v/v) hexane/1,2-dichloroethane/ethanol as eluent was studied.

***Stationary Phases.*** The CSP column of 5 cm L × 0.46 cm I.D. and 5 μm particle diameter purchased from Phenomenex (Torrance, CA, USA) was used in this study.





MARCEL DEKKER, INC.
270 Madison Avenue, New York, New York 10016

***Chemicals and Solvents.*** (*R*)-(+)-1,1′-Bi-2-naphthol (*R*-form, 99% pure, formula weight 286.33), (*S*)-(−)-1,1′-bi-2-naphthol (*S*-form, 99% pure, formula weight 286.33), and 1,3,5-tri-*tert*-butyl benzene (TTBB, 99%, formula weight 246.44) were purchased from Aldrich (Milwaukee, WI, USA). Hexane, 1,2-dichloroethane, and ethanol were purchased from Tedia (Fairfield, OH, USA).

## Apparatus

***Elution Chromatography.*** Our high performance liquid chromatographic system includes a Jasco Model PU980 solvent metering pump, a Jasco Model UV970 UV detector (Tokyo, Japan), and a Rheodyne Model 7125 6-way syringe loading valve fitted with a 20-mL sample loop (Cotati, CA, USA). The column and sample loop were thermostatted to the appropriate temperature in a circulating water bath. The millivolt signal from the detector was converted to digital form with the aid of an analog-to-digital interface card (Scientific Information Service Corp., Taiwan) interfaced with a microcomputer for data storage and processing.

***Frontal Chromatography.*** A schematic drawing of the frontal chromatographic system is shown in Fig. 1. The pump, UV detector, and water bath are the same as those used in the elution chromatographic system. Besides these, the system also includes a Valco Model E36 10-port electrically-actuated switching valve fitted with two 5-mL sample loops (Houston, TX,

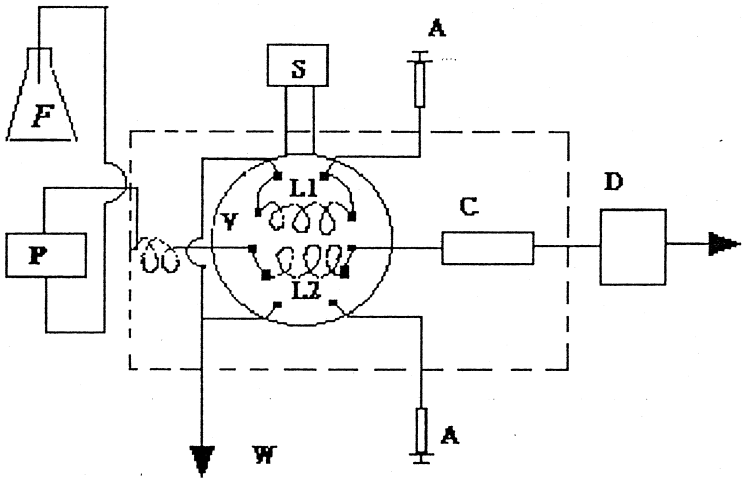


FIG. 1 Schematic diagram of the liquid chromatograph for isotherm measurements by frontal chromatography. P: solvent metering pump; F: solvent flask; V: 10-port swithing valve; L1, L2: 5-mL sample loops; S: electrical actuator; A: 25-mL needle injector; C: chiral column; D: UV detector; W: waste solvent; - - -: water bath.





MARCEL DEKKER, INC.
270 Madison Avenue, New York, New York 10016

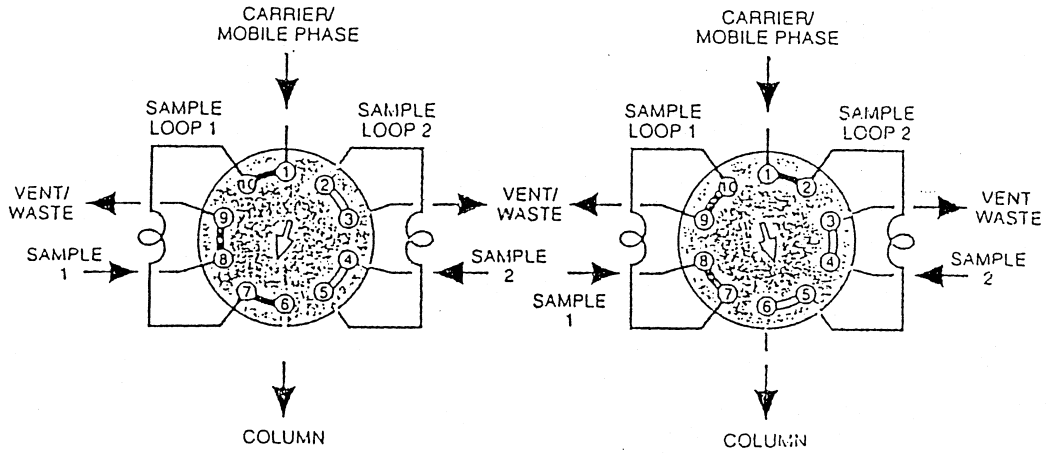


FIG. 2 Operating sequence of the 10-port switching valve (Valco Model E36).



USA), and a Jasco Model 970-02 preparative UV cell (Tokyo, Japan). The operating sequence of the 10-port valve is shown in Fig. 2.

Detecting conditions, such as wavelength, sensitivity, and light-path lengths, were chosen according to the concentration of the sample in the effluent.

## Procedures and Data Analysis

***Elution Chromatography.*** In the elution on a plateau (EP) method, the pulse-response experiments of the *R*-form and the *S*-form of 1,1′-bi-2-naphthol were carried out by using their solutions ranging in concentration from 0 to 0.024 M as the eluent. The volumetric flow rate of the eluent was varied in the range from 0.5 to 3.0 mL/min.

In this study, small concentration perturbation pulses were introduced into the carrier solvent flow including 1,1′-bi-2-naphthol. Each sample solution was prepared by adding a small amount of 1,1′-bi-2-naphthol into each corresponding carrier solvent. The difference in 1,1′-bi-2-naphthol concentration between the carrier solvent and the sample solution was very small. Therefore, the moment method based on the linear adsorption assumption could be used to analyze the experimental data.

The first moment and the variance were determined from the elution peaks by moment analysis. The measured peak time, $\mu_{1,\mathrm{exp}}$, was corrected to be the first moment by Eq. (6) with $V_e = 0.0476$ mL in this system.

When straight lines through the origin are observed in plots of $\mu_1$ vs $L/v_s$ at various eluent concentrations, according to Eq. (3) the differential equilibrium constants, $K$, can be calculated by the slopes of their corresponding straight lines. Furthermore, when the adsorption equilibrium behavior of the system is



MARCEL DEKKER, INC.
270 Madison Avenue, New York, New York 10016

correlated properly by the Langmuir equation, Eq. (1), $K$ can be calculated by

$$K = \frac{a}{(1 + bC)^2} \tag{8}$$

which can be further linearized by

$$\left(\frac{1}{K}\right)^{\frac{1}{2}} = \frac{1}{a^{\frac{1}{2}}} + \frac{b}{a^{\frac{1}{2}}} C \tag{9}$$

i.e., the experimental data be fitted by the linear plot of $(1/K)^{1/2}$ vs $C$. The slope ($b/a^{1/2}$) and intercept ($1/a^{1/2}$) of this plot can then be used to calculate the two model parameters of the Langmuir equation, $a$ and $b$.

Also, when straight lines are observed in Van Deemter plots of HETP vs $v$ at various eluent concentrations, according to Eq. (4b) the overall mass transfer coefficients, $k$, and the axial dispersion coefficients, $D_L$, can be obtained by the slopes and intercepts of their corresponding straight lines.

***Measurement of the Bed Porosity.*** The bed porosity includes the particle porosity, $\varepsilon_p$, the column porosity, $\varepsilon$, and the total bed porosity, $\varepsilon_t$. The relationship among them is as follows:

$$\varepsilon_t = \varepsilon + (1 - \varepsilon)\varepsilon_p \tag{10}$$

$\varepsilon_t$ was measured in a similar manner by the pulse-response experiments of 1,3,5-tri-*tert*-butyl benzene (TTBB), which is nonadsorbable on the Pirkle D-phenylglycine CSP column. The volumetric flow rate of the eluent, which was neat, was varied in the range from 0.5 to 3.0 mL/min.

According to Eq. (3a), the total bed porosity, $\varepsilon_t$, can be calculated by the mean residence time of TTBB, $t_{or}$, as

$$t_{or} = \frac{L}{v_s}[\varepsilon + (1 - \varepsilon)\varepsilon_p] = \frac{L}{v_s}\varepsilon_t \tag{11}$$

When a straight line through the origin is observed in a plot of $t_{or}$ vs $L/v_s$, $\varepsilon_t$ can be calculated by the slope of the straight line according to Eq. (11).

***Frontal Chromatography.*** The frontal analysis (FA) method was carried out with the instrument shown in Fig. 1 by the following procedure. First, the column was equilibrated with the eluent. The eluent was passed through loop $L_2$ into the column, and loop $L_1$ was loaded with 5 mL of sample with the lowest solute concentration. The 10-way valve was switched on electrically so that the column was perfused with the sample solution from loop $L_1$, and frontal development took place. Loop $L_2$ was then loaded with sample solution with the next higher concentration and, after the concentration of the first sample reached a plateau in frontal development, the valve was switched again to introduce the next sample. By this sequence, samples with increasing con-

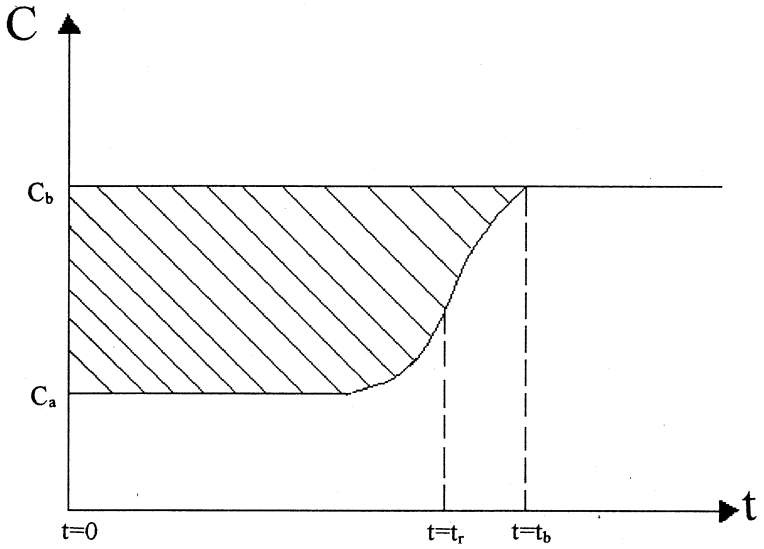


FIG. 3 Illustration of the frontal chromatogram used in the calculation of the equilibrium surface concentration.

centrations were introduced into the column sequentially until the sample of the highest concentration was chromatographed. Thereafter, neat eluent was pumped through the column.

Figure 3 shows the frontal chromatogram as the solute concentration from $C_a$ to $C_b$, which are the concentrations in the eluent at the beginning and the end of frontal development, respectively. The sample is introduced at $t = 0$ and equilibrium is reached at $t = t_b$. The overall mass balance of the column between $t = 0$ and $t = t_b$ can be expressed as

$$\int_0^{t_b} (C_b - C_{exit})\, Q_f\, dt = V_o\,(C_b - C_a) + V_a\,(q'_b - q'_a) \qquad (12a)$$

where $C_{exit}$ is the exit concentration (mmol/mL of solution); $q'_a$ and $q'_b$ [mmol/mL of adsorbent (without pores)] are the surface concentrations in equilibrium with the solute concentrations $C_a$ and $C_b$, respectively; $Q_f$ is the volumetric flow rate of the eluent; $V_o$ is the hold-up volume of the column, and $V_a$ is the volume of the CSP adsorbent in the column (excluding the pore volume). By letting $V_t$ be the total volume of the column, $V_o$ and $V_a$ can be calculated by $V_o = V_t\varepsilon_t$ and $V_a = V_t(1 - \varepsilon_t)$, respectively. When the shaded area in Fig. 3 is approximately equal to a rectangular area in the same concentration range and with time from $t = 0$ to $t = t_r$, Eq. (12a) can be simplified as

$$V_r(C_b - C_a) = V_o(C_b - C_a) + V_a(q'_b - q'_a) \qquad (12b)$$

where $V_r$ is the mean retention volume of the front corresponding to concentration $C_b$, which can be calculated by $V_r = Q_f t_r$, with $t_r$ being the corre-

sponding mean retention time. By repeating the above calculation procedure, all the equilibrium solute concentrations ($q'$) corresponding to their solute concentrations ($C$) can be obtained. Also, letting the unit of $q$ be mmol/mL of adsorbent (with pores), which is more commonly adopted, $q'$ can be further transformed into $q$ by $q = q'(1 - \varepsilon_p)$.

When the adsorption equilibrium behavior of the system is correlated properly by the Langmuir equation, Eq. (1) can be linearized to

$$q^{-1} = \frac{1}{a} C^{-1} + \frac{b}{a} \tag{13}$$

i.e., the experimental data can be fitted by the linear plot of $q^{-1}$ vs $C^{-1}$. The slope ($1/a$) and intercept ($b/a$) of this plot can then be used to calculate the two model parameters of the Langmuir equation, $a$ and $b$. Alternatively, since the data of $q$ vs $C$ are directly available from this method, the two model parameters can also be determined by nonlinear regression software, e.g., a simplex algorithm (17) available on Matlab (The Math Work Inc., Natick, MA, USA).

## RESULTS AND DISCUSSION

### Measurement of the Bed Porosity

The retention times, $t_{or}$, were measured for TTBB in this CSP column over a range of eluent flow rates (1.0, 1.5, 2.0, 2.5 mL/min) and plotted against $L/v_s$, as shown in Fig. 4, where a straight line through the origin was observed. According to Eq. (11), the slope of the linear plot yields $\varepsilon_t = 0.80$.

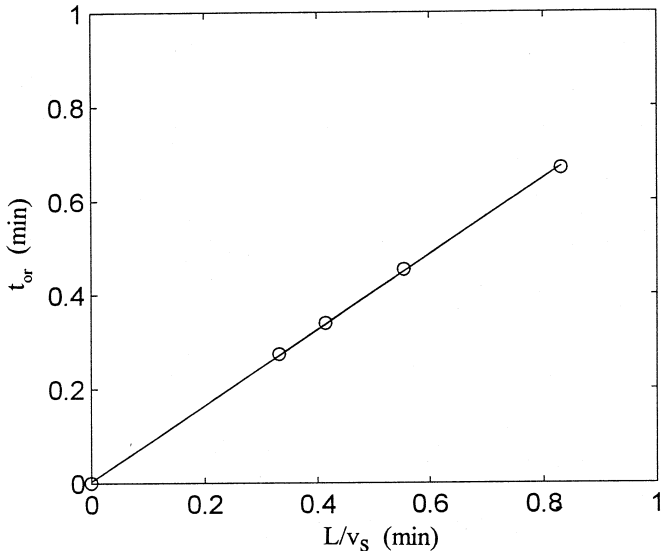


FIG. 4 Plot of retention time vs $L/v_s$ for TTBB at neat eluent.





MARCEL DEKKER, INC.
270 Madison Avenue, New York, New York 10016

Also, the data for $\varepsilon_p = 0.50$ provided by Phenomenex (Torrance, CA, USA) were used. By substituting the values of $\varepsilon_t$ and $\varepsilon_p$ into the $\varepsilon_t = \varepsilon + (1 - \varepsilon)\varepsilon_p$ equation, $\varepsilon$ was derived as 0.60.

## The Elution on a Plateau (EP) Method

Figures 5(a) and 5(b) show the chromatograms measured from the pulse response experiments of the *R*-form and the *S*-form of 1,1′-bi-2-naphthol, respectively, at four flow rates (1.0, 1.5, 2.0, 2.5 mL/min) of neat eluent (zero solute concentration) and a temperature of 30°C. The same experiments were run with stepwise increases of the eluent concentration to 0.024 mmol/mL (or

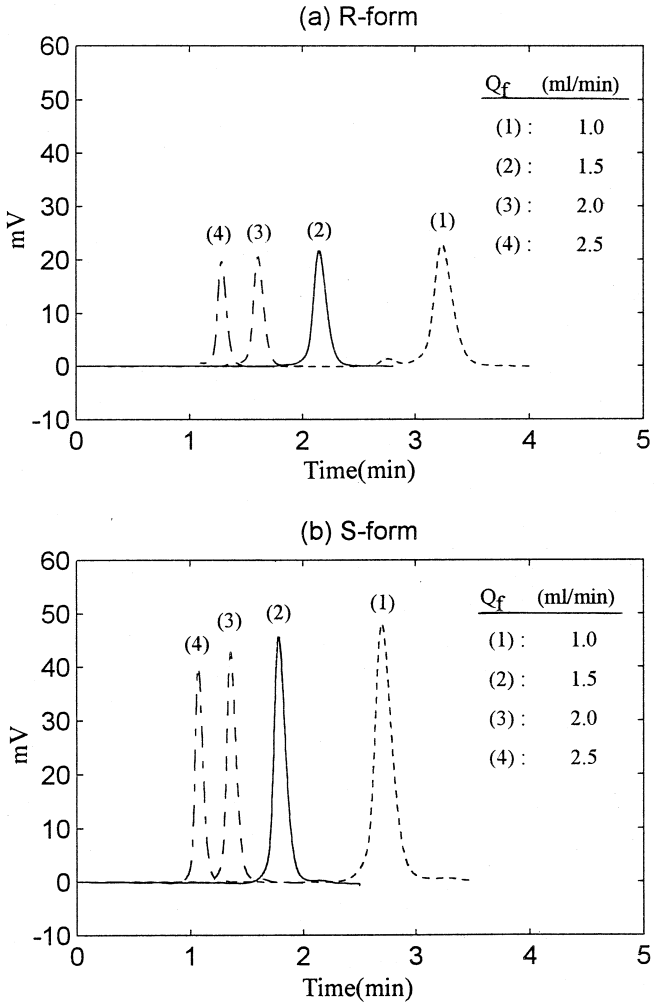


FIG. 5 The EP method: chromatographic peaks of 1,1′-bi-2-naphthol. Conditions: mobile phase, neat; temperature, 30°C; flow rate, as indicated.





MARCEL DEKKER, INC.
270 Madison Avenue, New York, New York 10016

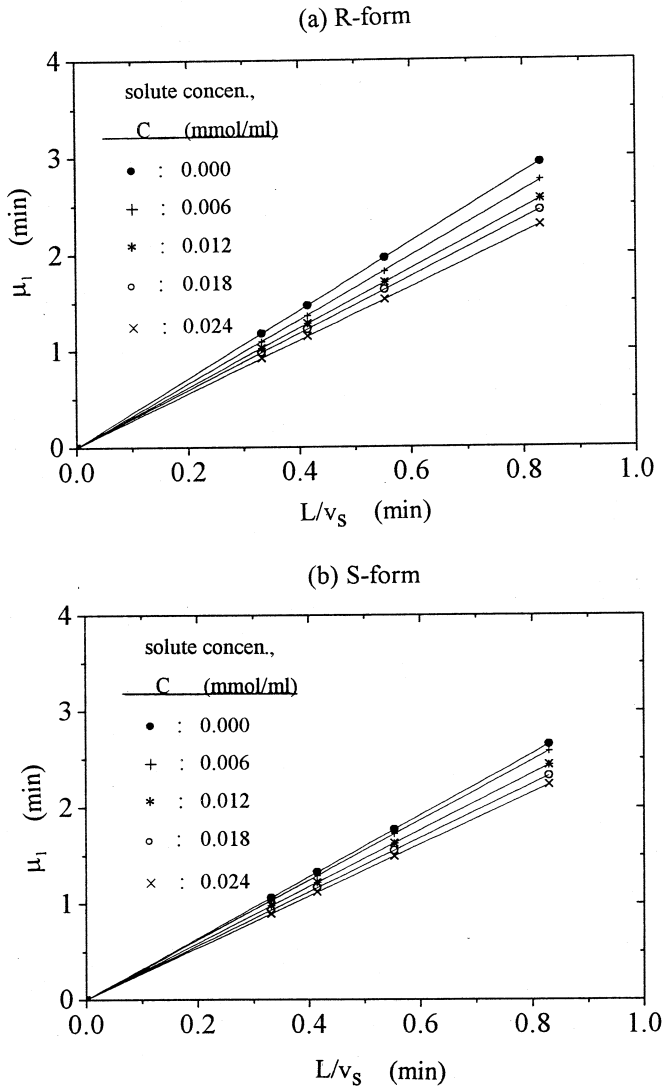


FIG. 6 The EP method: plots of first moment vs $L/v_s$ for 1,1′-bi-2-naphthol. Best linear fits of the experimental data are given by the solid lines. Other condition: temperature, 30°C.

M). In order to test the reproducibility of this method, three replicates were run for each concentration.

The experimental data plotted as $\mu_1$ vs $L/v_s$ at various solute concentrations, as shown in Figs. 6(a) and 6(b) for the *R*-form and the *S*-form, respectively, fitted quite well into a set of straight lines through the origin. It is noted that the reproducibility of $\mu_1$ was so good that the deviation for $\mu_1$ is not shown in these figures. The differential equilibrium constants, *K*, of the *R*-form and the *S*-form at their corresponding eluent concentrations were calcu-

TABLE 1
The Differential Equilibrium Constants, $K$, Calculated by the EP Method

| Solute concentration, $C$ (M) | $K$ [mL of solution/mL of adsorbent (with pores)] | |
|---|---|---|
| | $R$-form | $S$-form |
| 0.000 | 6.84 | 5.97 |
| 0.006 | 6.20 | 5.75 |
| 0.012 | 5.69 | 5.33 |
| 0.018 | 5.35 | 4.99 |
| 0.024 | 4.89 | 4.71 |



lated from the slopes of their corresponding linear plots by using Eq. (3) and are shown in Table 1.

Figure 7 shows the data of Table 1 plotted as $(1/K)^{\frac{1}{2}}$ vs $C$ (the solute concentration) for the $R$-form and the $S$-form. They deviated slightly ($R^2 = 0.996$ and 0.990 for the $R$-form and the $S$-form, respectively) from fitting straight lines, and the Langmuir model was reasonably adopted to describe the adsorption behavior of each isomer. The parameters of the Langmuir model calculated from the slopes and the intercepts of the above linear plots for the $R$-form and the $S$-form are as follows: $a_R = 6.75$, $b_R = 7.60$, $a_S = 6.04$, $b_S =$

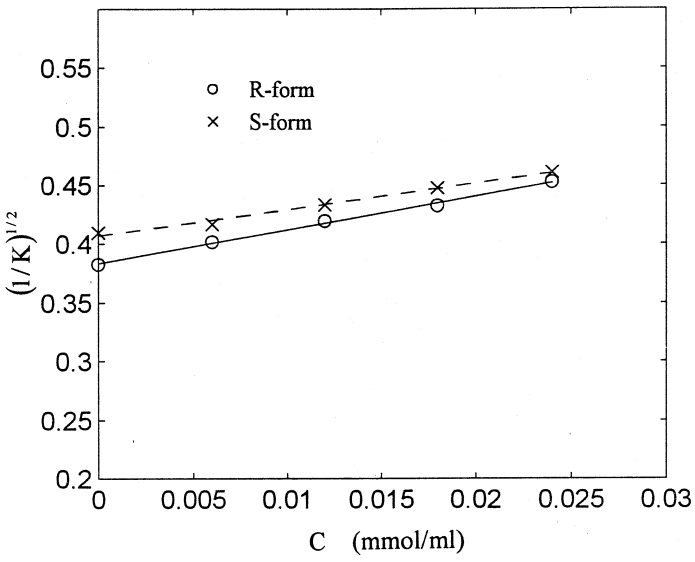


FIG. 7 The EP method: plot of $(1/K)^{\frac{1}{2}}$ vs solute concentration for 1,1′-bi-2-naphthol. The lines are the best linear fits of the experimental data. Other condition: temperature, 30°C.



MARCEL DEKKER, INC.
270 Madison Avenue, New York, New York 10016

5.46. The units of *a* and *b* are mL of solution/mL of adsorbent (with pores) and mL of solution/mmol, respectively. Finally, the separation factor, $\alpha$, is calculated as

$$\alpha|_{EP} = a_R/a_S = 1.12 \tag{14}$$

The experimental data for both the *R*-form and the *S*-form plotted as HETP vs *v* (Van Deemter plot) at zero solute concentration are shown in Fig. 8. The effect of the solute concentration on HETP was found to be relatively small for the region being studied (0.000–0.024 M) and is not shown in this plot. It should be noted that due to the unstable baseline signal detected, especially for the cases of high solute concentrations, the calculated HETP data were not as reproducible as those of $\mu_1$. The HETP values of the *S*-form did not differ much (only slightly higher) from those of the *R*-form, and their theoretical plates (HETP) were between 0.003 and 0.005 cm for the flow rate region being studied. The slopes of both lines in this plot are quite low, which means the mass transfer resistance of each isomer inside the 5-$\mu$m CSP particle is therefore very small. As the above data were linearly fitted to Eq. (4b), the averaged values of the overall mass transfer coefficients, *k*, and the axial mixing constant, $\lambda$, were calculated to be $k = 3200$ 1/min and $\lambda = 0.001$ cm. These parameters will be used for both the *R*-form and the *S*-form in our future simulation of system performance.

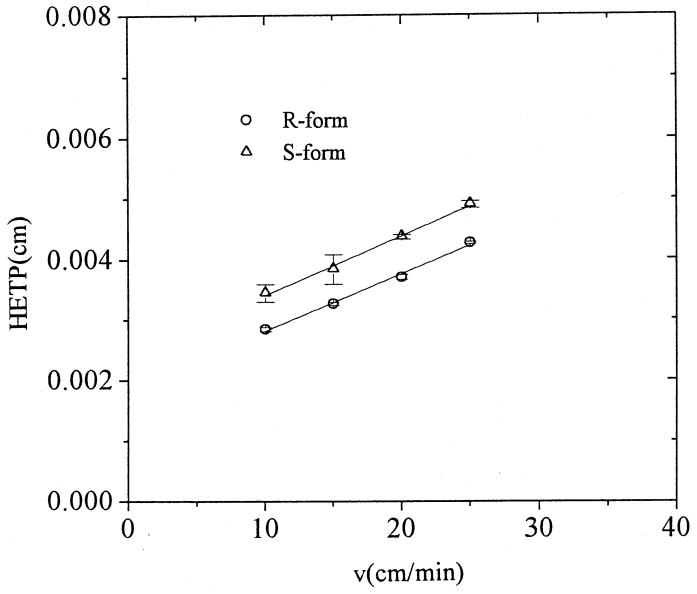


FIG. 8 The EP method: plot of HETP vs *v* for 1,1′-bi-2-naphthol at neat eluent. ——: Best linear fits of the experimental data. Other condition: temperature, 30°C. Error bars span 2 standard deviations.





MARCEL DEKKER, INC.
270 Madison Avenue, New York, New York 10016

## The Frontal Analysis (FA) Method

First, the experiments were performed at an eluent flow rate of 1.0 mL/min and a temperature of 30°C. Figures 9(a) and 9(b) show the chromatograms measured from the step response experiments of the *R*-form and the *S*-form, respectively, as the solute concentration increased from 0.000 to 0.024 M. Again, in order to test the reproducibility of this method, the same set of experiment was repeated three times. The amount adsorbed, $q$, at various solute concentrations can be directly calculated by Eq. (12b). The results of three replicates of the *R*-form are shown in Table 2 as a calculation example. This method was found to be very reproducible, as shown in Table 2 by the small standard deviations for the equilibrium surface concentrations.



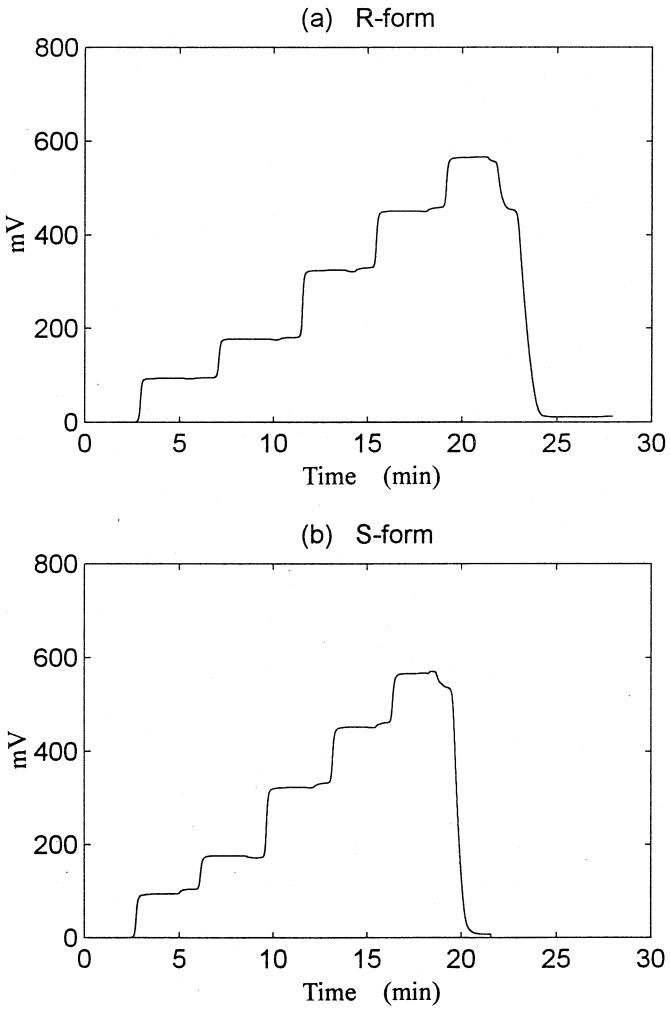


FIG. 9 The FA method: frontal chromatogram of 1,1′-bi-2-naphthol. Conditions: temperature, 30°C; flow rate, 1 mL/min.



MARCEL DEKKER, INC.
270 Madison Avenue, New York, New York 10016

TABLE 2
Calculation of the Equilibrium Surface Concentrations of the *R*-Isomer by the FA Method. Conditions: Temperature, 30°C; Flow Rate, 1 mL/min; Three Replicates

| Solute concentration, $C$(M) | Injection time (minutes) | Mean frontal appearing time (minutes) | Mean retention time, $t_r$ (minutes) | Mean retention volume, $V_r$ (mL) | Equilibrium surface concentration, $q$ | Mean of equilibrium surface concentration, $\bar{q}$ | Standard deviation of $q$ |
|---|---|---|---|---|---|---|---|
| 0.003 | 0.060 | 2.9361 | 2.8761 | 2.8761 | 0.01996 | | |
| | 0.069 | 2.9613 | 2.8923 | 2.8923 | 0.02011 | 0.02009 | 0.00012 |
| | 0.064 | 2.9660 | 2.9020 | 2.9020 | 0.02019 | | |
| 0.006 | 4.350 | 7.1099 | 2.7599 | 2.7599 | 0.03887 | | |
| | 4.331 | 7.0941 | 2.7631 | 2.7631 | 0.03905 | 0.03905 | 0.00018 |
| | 4.790 | 7.5638 | 2.7738 | 2.7738 | 0.03923 | | |
| 0.012 | 8.970 | 11.5931 | 2.6231 | 2.6231 | 0.07423 | | |
| | 8.108 | 10.7201 | 2.6121 | 2.6121 | 0.07420 | 0.07430 | 0.00014 |
| | 9.135 | 11.7513 | 2.6163 | 2.6163 | 0.07446 | | |
| 0.018 | 13.008 | 15.5124 | 2.5044 | 2.5044 | 0.10744 | | |
| | 12.187 | 14.6717 | 2.4847 | 2.4847 | 0.10706 | 0.10735 | 0.00026 |
| | 13.141 | 15.6388 | 2.4978 | 2.4978 | 0.10756 | | |
| 0.024 | 16.821 | 19.2098 | 2.3888 | 2.3888 | 0.13856 | | |
| | 17.422 | 19.8075 | 2.3855 | 2.3855 | 0.13812 | 0.13841 | 0.00025 |
| | 17.225 | 19.6061 | 2.3811 | 2.3811 | 0.13854 | | |



Then the effect of flow rate for the system was investigated. Figure 10 shows isotherms of the *R*-form and the *S*-form measured for flow rates of 0.5, 1.0, and 1.5 mL/min. There is apparently nearly no change in the isotherm shape over this flow-rate range. The eluent flow rate was then fixed at 1.0 mL/min for the following measurements.

Figure 11 shows the isotherm data plotted as $1/q$ vs $1/C$ for the *R*-form and the *S*-form. They fitted quite well into the straight lines ($R^2 > 0.999$ for both the *R*-form and the *S*-form). Again, the Langmuir model was confirmed to be the right one to describe the adsorption behavior of each isomer. The parameters of the Langmuir model calculated from the slopes and the intercepts of the above linear plots for the *R*-form and the *S*-form are as follows: $a_R = 6.74$, $b_R = 6.93$, $a_S = 6.13$, $b_S = 5.97$, where the units of $a$ and $b$ are the same as before. Finally, the separation factor, $\alpha$, is calculated as

$$\alpha|_{FA} = a_R/a_S = 1.10 \quad (15)$$

## Comparison between Both Methods

Figure 12 shows the comparison of the fitted adsorption isotherms of the *R*-form and the *S*-form obtained from both methods. It can be seen that they are



MARCEL DEKKER, INC.
270 Madison Avenue, New York, New York 10016

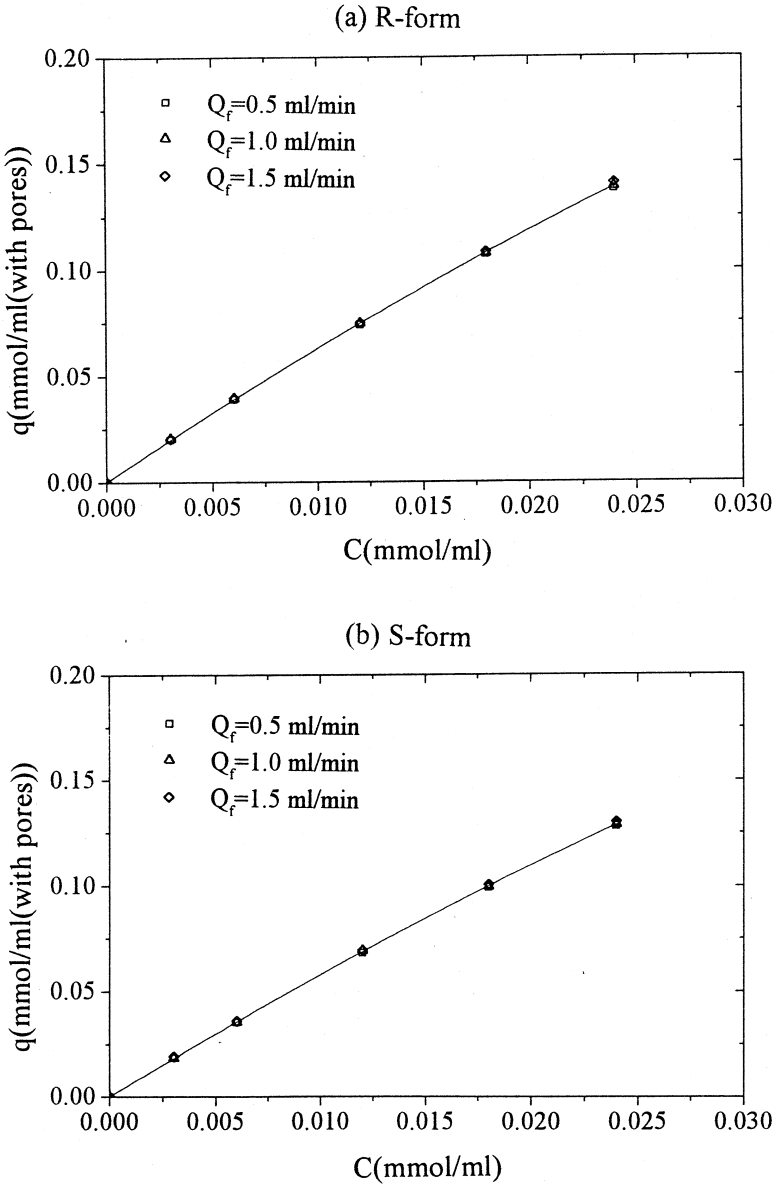


FIG. 10 The FA method: adsorption isotherms measured at different flow rates. Best fits of the experimental data to the Langmuir equation are given by the solid lines. Other condition: temperature, 30°C.

in good agreement for both components in the region of solute concentration below 0.015 M, but are slightly different, with errors within about 5%, in the region of solute concentration higher than 0.015 M.

The EP method was found to have the following operating difficulties: significant detection problems at high concentrations, perturbation size can influence the accuracy of the result, solute consumption is substantial, and the

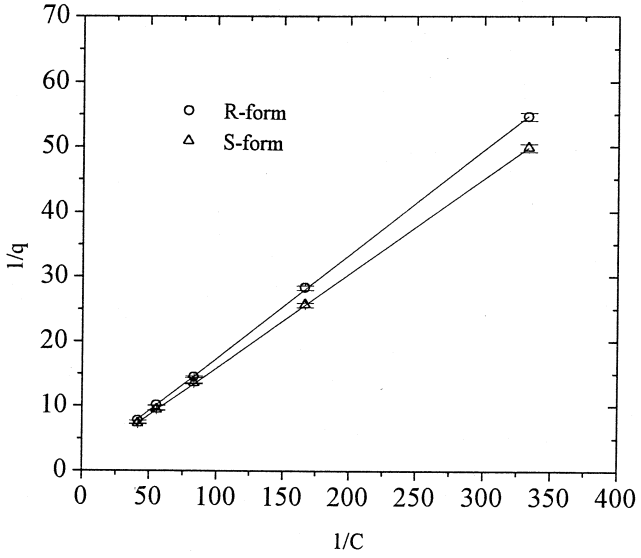


FIG. 11 The FA method: plot of $1/q$ vs $1/C$ for 1,1′-bi-2-naphthol. ——: Best linear fits of the experimental data. Conditions: temperature, 30°C; flow rate, 1 mL/min. Error bars span 2 standard deviations.



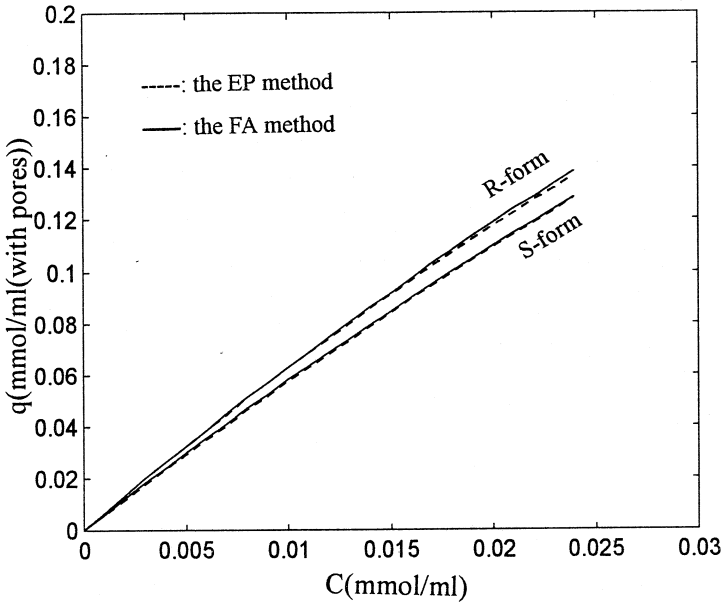


FIG. 12 Comparison of the adsorption isotherms between the EP and FA methods. Condition: temperature, 30°C.



MARCEL DEKKER, INC.
270 Madison Avenue, New York, New York 10016

experimental complexity is greater than that for the FA method. In contrast, the FA method, measuring the equilibrium surface concentration directly, was found to be more reliable and easier to operate than the EP method for isotherm measurement. Also, if self-packed narrow-bore columns are available and used in the FA method, much less time and material than is required

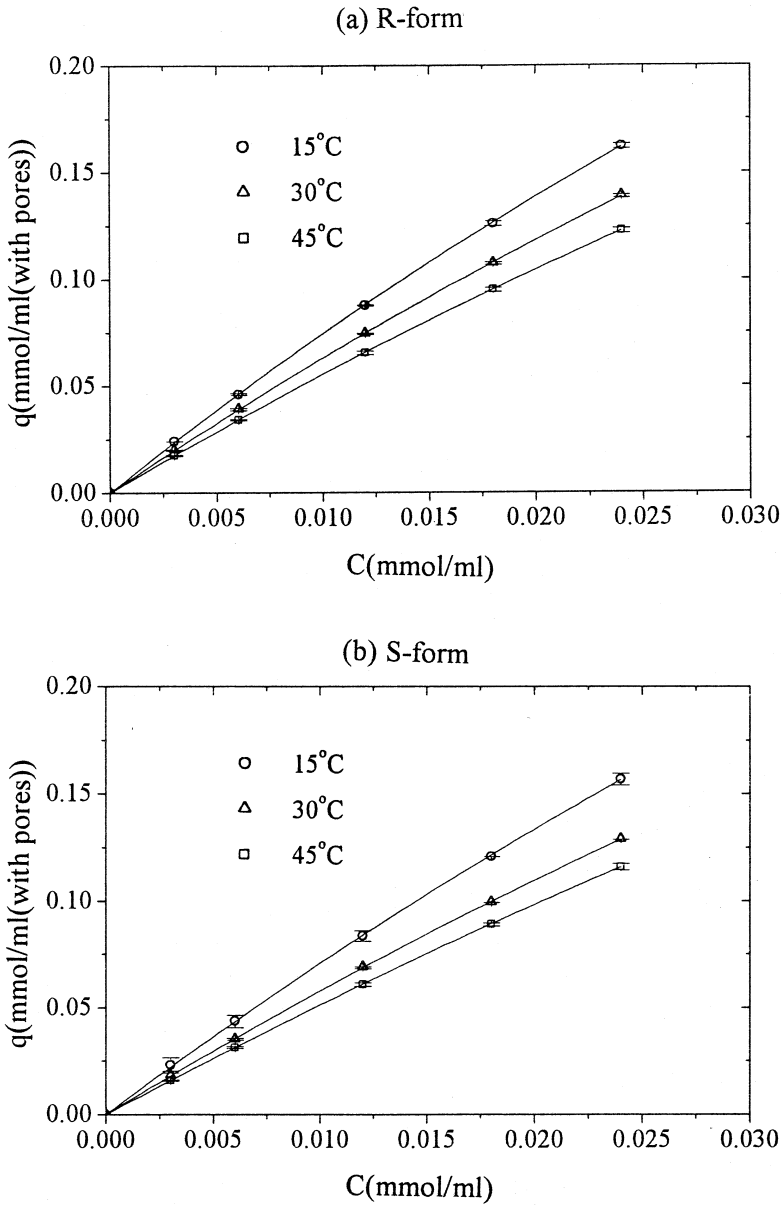


FIG. 13 Isotherms illustrating the effect of temperature on the adsorption of 1,1′-bi-2-naphthol on Pirkle covalent D-phenylglycine. Best fits of the experimental data to the Langmuir equation are given by the solid lines. Other condition: flow rate, 1 mL/min. Error bars span 2 standard deviations.





MARCEL DEKKER, INC.
270 Madison Avenue, New York, New York 10016

for the EP method can be expected. Therefore, the FA method was selected as the more rapid, precise, and accurate measurement method. However, the unique advantage of the EP method is that it can be easily used to measure other adsorption characteristics, e.g., the axial dispersion coefficient and the diffusion coefficient of each solute, besides the equilibrium isotherm.

## Effect of Temperature on Adsorption Isotherms

The FA method was then used to measure the adsorption isotherms of the *R*-form and the *S*-form at some other temperatures. Isotherms of the *R*-form and the *S*-form at 15, 30, and 45°C are shown and compared in Fig. 13, and their corresponding Langmuir parameters are given in Table 3, which were correlated directly by nonlinear regression. Again, the reproducibility was reasonably good and the isotherm data were fitted well by the Langmuir model for all three temperatures, as shown in Table 3 by the small standard deviations for parameters *a* and *b*. The right pattern of a decrease in adsorption with increasing temperature was found for both the *R*-form and the *S*-form. Table 3 also shows the separation factors at these three temperatures. Apparently the separation factor was not improved by decreasing or increasing the operating temperature away from 30°C, which suggests that the optimal operating temperature is around 30°C.

Isosteric heat of adsorption, $Q_{st}$, was obtained from isotherms at the above three different temperatures by using the Clausius–Clapeyron equation:

$$d \ln C/d(1/T) = Q_{st}/R_g \tag{16}$$

Also, $Q_{st}$ for zero surface coverage, $Q_{st,0}$, was determined by the van't Hoff equation:

$$d \ln K_0/d(1/T) = -Q_{st,0}/R_g \tag{17}$$

TABLE 3
Langmuir Parameters and the Separation Factor for 1, 1′-Bi-2-naphthol on Pirkle Covalent D-Phenylglycine at 15, 30 and 45°C

| Temperature (°C) | Langmuir parameters | | | | Separation factor, α |
|---|---|---|---|---|---|
| | *R*-form | | *S*-form | | |
| | *a* ± SD | *b* ± SD | *a* ± SD | *b* ± SD | |
| 15 | 8.0357 ± 0.0596 | 7.9475 ± 0.4307 | 7.5275 ± 0.0947 | 6.4034 ± 0.7081 | 1.068 |
| 30 | 6.7350 ± 0.0447 | 6.9275 ± 0.3771 | 6.1320 ± 0.0381 | 5.9702 ± 0.3468 | 1.098 |
| 45 | 5.8901 ± 0.0212 | 6.3400 ± 0.2027 | 5.3729 ± 0.0184 | 4.6931 ± 0.1860 | 1.096 |





MARCEL DEKKER, INC.
270 Madison Avenue, New York, New York 10016

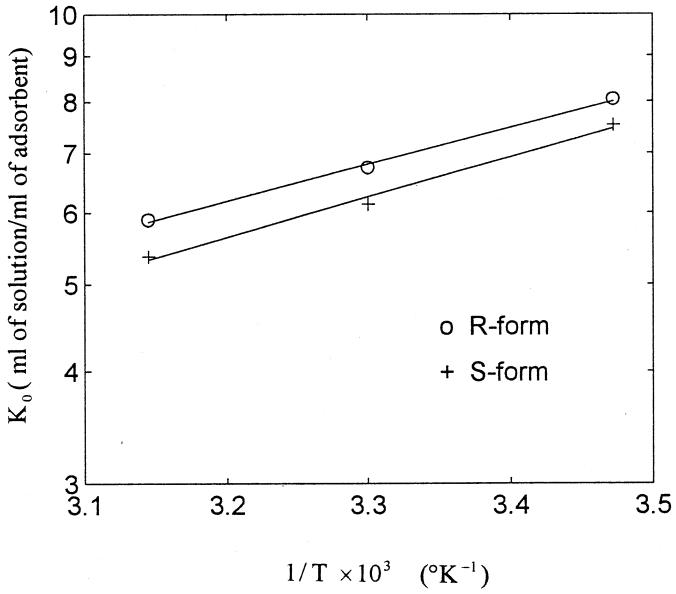


FIG. 14 van't Hoff plots of adsorption equilibrium constants at zero surface coverage (Henry's law constants) of 1,1′-bi-2-naphthol. ——: Best linear fits of the experimental data.

where $R_g$ is the gas constant and $K_0$ is the adsorption equilibrium constant at zero surface coverage or the so-called Henry's law constant. A plot of $\ln K_0$ vs $1/T$, as shown in Fig. 14, results in a reasonable linear fit ($R^2 = 0.997$ and 0.991 for the *R*-form and the *S*-form, respectively). According to Eq. (17), $Q_{st,0}$ was calculated to be 1.89 and 2.05 kcal/mol for the *R*-form and the *S*-form, respectively. Isosters for various amounts adsorbed are shown in Fig. 15. The corresponding isosteric heats of adsorption, $Q_{st}$, calculated by Eq. (16), are listed in Table 4. The isosteric heat of adsorption is about 1.9 to 2.1 kcal/mol for both the *R*-form and the *S*-form, regardless of the amount adsorbed. The nearly constant value of $Q_{st}$ suggests that Pirkle covalent D-phenylglycine has an energetically homogeneous surface.

## Prediction of Adsorption Isotherm for the Binary-Component System

Both the FA and EP methods can be extended for the measurement of competitive adsorption isotherms between enantiomers. However, they require a lot of experimental work which is very time-consuming and costly in terms of material required.

Instead, the binary-component adsorption equilibrium isotherms can be predicted from the single-component equilibrium isotherms by using the ideal adsorbed solution (IAS) model (18). Since the single-component isotherms can be accounted for by the Langmuir model, the two-term expansion series

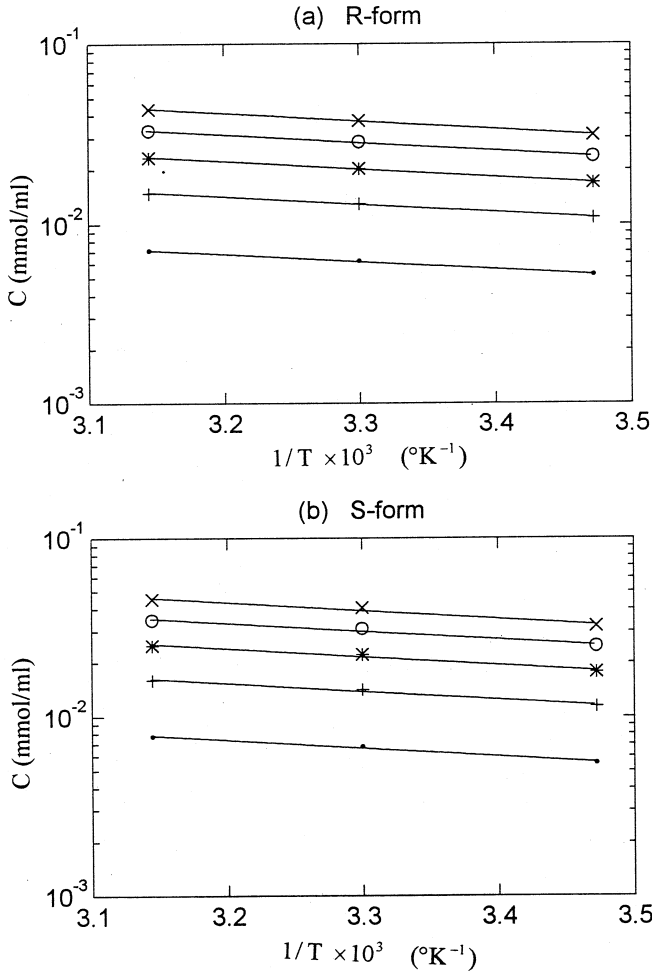


FIG. 15 Clausius–Clapeyron plots of adsorption isosteres of 1,1′-bi-2-naphthol. The symbols represent the following surface coverage concentrations: 0.04 (●), 0.08 (+), 0.12 (∗), 0.16 (❍), and 0.20 mmol/ml (×). Best linear fits of the experimental data are given by the solid lines.

TABLE 4
Isosteric Heat of Adsorption of 1,1′-Bi-2-naphthol on Pirkle Covalent D-Phenylglycine

| $q$ (mmol/mL of adsorbent) | $-Q_{st}$ (kcal/mol) | |
|---|---|---|
| | *R*-form | *S*-form |
| 0.00 | 1.89 | 2.05 |
| 0.04 | 1.91 | 2.06 |
| 0.08 | 1.93 | 2.06 |
| 0.12 | 1.96 | 2.07 |
| 0.16 | 1.99 | 2.08 |
| 0.20 | 2.02 | 2.09 |





MARCEL DEKKER, INC.
270 Madison Avenue, New York, New York 10016

of the Levan–Vermeulen isotherm (19), derived from the IAS model, can be used to calculate the binary-component adsorption equilibrium isotherms. The explicit form of the Levan–Vermeulen isotherm can be written as

$$q_R = \frac{q_{\text{sat}} b_R C_R}{1 + b_R C_R + b_S C_S} + \Delta_{R,S}$$
$$q_S = \frac{q_{\text{sat}} b_S C_S}{1 + b_R C_R + b_S C_S} - \Delta_{R,S} \tag{18}$$

where $q_{\text{sat}}$ and $\Delta_{R,S}$ are defined as follows:

$$q_{\text{sat}} = \frac{a_R C_R + a_S C_S}{b_R C_R + b_S C_S} \tag{19a}$$



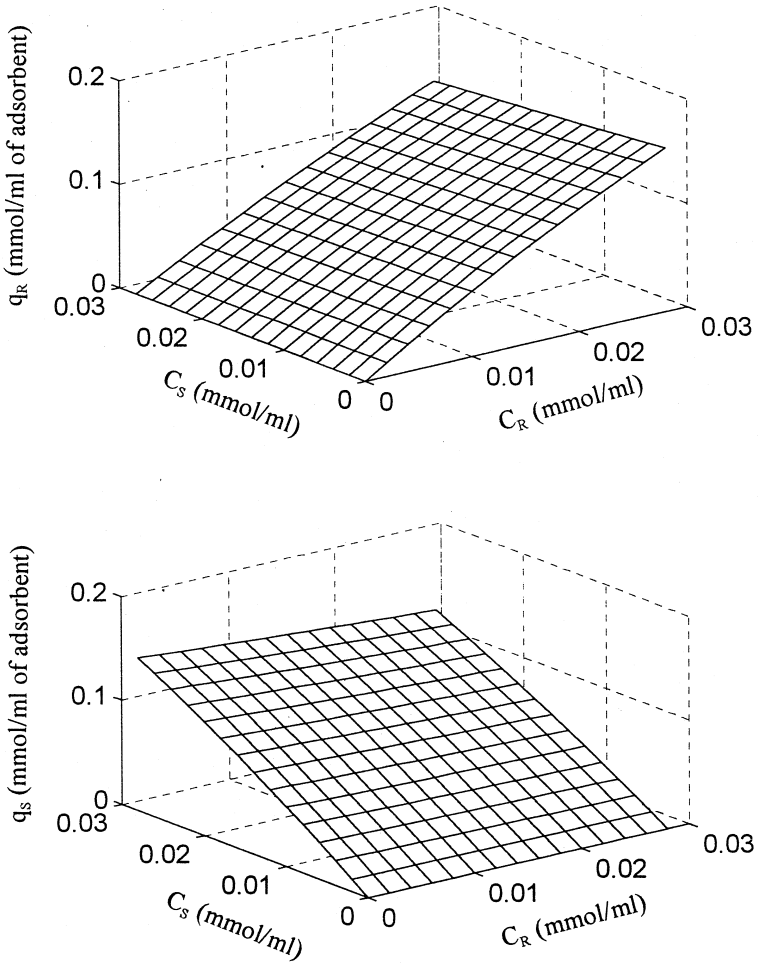


FIG. 16 Binary-component adsorption equilibrium isotherms for both isomers of 1,1′-bi-2-naphthol predicted by the Levan–Vermeulen model. Condition: temperature, 30°C.



MARCEL DEKKER, INC.
270 Madison Avenue, New York, New York 10016

$$\Delta_{R,S} = \left(\frac{a_R}{b_R} - \frac{a_S}{b_S}\right) \frac{b_R b_S C_R C_S}{(b_R C_R + b_S C_S)^2} \ln(1 + b_R C_R + b_S C_S) \qquad (19b)$$

and $a_R$, $a_S$, $b_R$, and $b_S$ are the four model parameters which can be provided from the above single-component adsorption isotherm measurements.

The binary-component adsorption equilibrium isotherm was calculated from the measured single-component Langmuir parameters by using the above model, which leads to the results shown in Fig. 16 and will be used for our future simulation of system performance.

## CONCLUSIONS

This study measured the adsorption characteristics of 1,1′-bi-2-naphthol on Pirkle-type (3,5-dinitrobenzoyl phenylglycine covalently bonded to silica gel) chiral columns. The single-component isotherm of each isomer (including the *R*-form and the *S*-form) was measured by the elution on a plateau (EP) and the frontal analysis (FA) methods. The results showed that the *R*-form is more retained than the *S*-form, and the separation factor between them is about 1.1. The adsorption behavior of each isomer conforms to the Langmuir model in the concentration range studied. From single-component adsorption equilibrium isotherms, binary-component equilibrium data were calculated by the Levan and Vermeulen model based on the ideal adsorbed solution (IAS) theory.

In contrast, the isotherm data obtained by the FA and EP methods are in good agreement with errors within about 5% for both components. The FA method was more reliable, was easier to operate and required less time and material than the EP method. Therefore, the FA method was selected as the more rapid, precise, and accurate method for isotherm measurement.

The effect of temperature on adsorption isotherms was investigated by the FA method. The separation factor was relatively high around 30°C, at which temperature the system is suggested to be operated. The isosteric heat of adsorption was found to be about 2.0 kcal/mol for both the *R*-form and the *S*-form. The constant value of isosteric heat of adsorption, regardless of the amount adsorbed, concluded that Pirkle covalent D-phenylglycine has an energetically homogeneous surface.

The other adsorption characteristics were measured by the EP method. The HETP for both isomers were between 0.003 and 0.005 cm for the flow-rate region being studied. The averaged values of the overall mass transfer coefficients, $k$, and the axial mixing constant, $\lambda$, were calculated to be $k = 3200$ 1/min and $\lambda = 0.001$ cm, which will be used for both the *R*-form and the *S*-form in our future simulation of system performance.

## ACKNOWLEDGMENT

The authors thank the National Science Council of the Republic of China for the financial support received under Grant NSC 86-2214-E-224-001.

## REFERENCES

1. S. Ahuja (Ed.), *Chiral Separation by Liquid Chromatography*, American Chemical Society, Washington, DC, 1991.
2. G. Subramanian (Ed.), *Preparative and Process-Scale Liquid Chromatography*, Ellis Horwood, New York, NY, 1991.
3. P. C. Wankat, *Large Scale Adsorption and Chromatography*, CRC Press, Boca Raton, FL., 1986.
4. G. Ganetsos and P. E. Barker (Eds.), *Preparative and Production Scale Chromatography*, Dekker, New York, NY, 1993.
5. C. Rosini, L. Franzini, A. Raffaelli, and P. Salvadori, "Synthesis and Applications of Binaphthylic $C_2$-Symmetry Derivatives as Chiral Auxiliaries in Enantioselective Reactions," *Synthesis*, pp. 503–517 (1992).
6. K. Hattori and H. Yamamoto, "Asymmetric Aza-Diels-Alder Reaction: Enantio- and Diastereoselective Reaction of Imine Mediated by Chiral Lewis Acid," *Tetrahedron*, *49* (9), 1749–1760 (1993).
7. W. Fritz and E.-U. Schluender, "Simultaneous Adsorption Equilibria of Organic Solutes in Dilute Aqueous Solutions on Activated Carbon," *Chem. Eng. Sci*., *29*, 1279–1291(1974).
8. L. Jossens, J. M. Prausnitz, W. Fritz, E.-U. Schluender, and A. L. Myers, "Thermodynamics of Multi-solute Adsorption from Dilute Aqueous Solutions," *Ibid*., *33*, 1097–1112 (1978).
9. K. Miyabe and M. Suzuki, "Chromatography of Liquid-Phase Adsorption on Octadecylsilyl-Silica Gel," *AIChE J*., *38*(6), 901–910 (1992).
10. M. Martinez, A. Carrancio, J. L. Casillas, and J. Aracil, "Evaluation of Kinetic and Thermodynamic Parameters of Amino Acids on Midified Divinylbenzene-Polystyrene Resins Using a Liquid Chromatography Technique," *Ind. Eng. Chem. Res*., *34*(12), 4486–4493 (1995).
11. B.-G. Lim and C.-B. Ching, "Characterization of Chiral Adsorbents on the Chromatographic Separation of Praziquantel Enantiomers," *Ibid*., *35*(1), 169–175, (1996).
12. J. Jacobson, J. Frenz, and C. Horvath, "Measurement of Adsorption Isotherms by Liquid Chromatography," *J. Chromatogr*., *316*, 53–68 (1984).
13. J.-X. Huang and C. Horvath, "Adsorption Isotherms on High-Performance Liquid Chromatographic Sorbents," *Ibid*., *406*, 275–284 (1987).
14. H. Guan and G. Guiochon, "Properties of Some $C_{18}$ Stationary Phases for Preparative Liquid Chromatography," *Ibid*., *687*, 179–200 (1994).
15. D. M. Ruthven, *Principles of Adsorption and Adsorption Processes*, Wiley, New York, NY, 1984.
16. D. J. Gunn, "Axial and Radial Dispersion in Fixed Beds," *Chem. Eng. Sci*., *42*, 363–375 (1987).
17. J. A. Nelder and R. Mead, "A Simplex Method for Function Minimization," *Comput. J*., *7*, 308–313 (1964).
18. A. L. Myers and J. M. Prausnitz, "Thermodynamics of Mixed-Gas Adsorption," *AIChE J*., *11*, 121–127 (1965).
19. M. D. Levan and T. Vermeulen, "Binary Langmuir and Freundlich Isotherms for Ideal Adsorbed Solutions," *J. Phys. Chem*., *85*(22), 3247–3250 (1981).

*Received by editor April 3, 1998*
*Revision received May 1999*

# Request Permission or Order Reprints Instantly!